Journal of Nuclear Materials 393 (2009) 418–424

Contents lists available at ScienceDirect

Journal of Nuclear Materials

journal homepage: www.elsevier.com/locate/jnucmat

Phase transformation in δ-Pu alloys at low temperature: An in situ microstructural characterization using X-ray diffraction

B. Ravat *, C. Platteau, G. Texier, B. Oudot, F. Delaunay

CEA, Valduc, F-21120 Is-sur-Tille, France

ARTICLE INFO

Article history:
Received 25 September 2008
Accepted 24 June 2009

ABSTRACT

In order to investigate the martensitic transformation, an isothermal hold at −130 °C for 48 h was performed on a highly homogenized PuGa alloy. The modifications of the microstructure were characterized in situ thanks to a specific tool. This device was developed at the CEA–Valduc to analyze the crystalline structure of plutonium alloys as a function of temperature and more especially at low temperature using X-ray diffraction. The analysis of the recorded diffraction patterns highlighted that the martensitic transformation for this alloy is the result of a direct $\delta \rightarrow \alpha' + \delta$ phase transformation. Moreover, a significant Bragg's peaks broadening corresponding to the δ-phase was observed. A microstructural analysis was made to characterize anisotropic microstrain resulting from the stress induced by the unit cell volume difference between the δ and α′ phases. The amount of α′-phase evolved was analyzed within the framework of the Avrami theory in order to characterize the nucleation process. The results suggested that the growth mechanism corresponded to a general mechanism where the nucleation sites were in the δ-grain edges and the α′-phase had a plate-like morphology.

1. Introduction

Plutonium metal has six different phases between room temperature and its melting point (640 °C) at ambient pressure. Under ambient conditions, the thermodynamically stable phase of pure plutonium is the brittle α-phase (monoclinic structure). However, the high-temperature δ-phase (face-centered cubic structure), stable from 319 to 451 °C, can be held at room temperature by alloying plutonium with a few atomic percents of a so-called "δ-phase stabilizer" elements such as gallium, aluminum, cerium, or americium. For instance, for Pu–Ga systems at ambient condition, according to Chebotarev et al. [1], the δ-phase is metastable and gives rise to extremely slow eutectoid decomposition to $\alpha + Pu_3Ga$. When the metastable δ-phase is cooled down to sub-ambient temperature, a partial transformation to the α′-martensitic phase occurs. The crystallographic structure of the α′-phase is similar to the monoclinic α-phase with slightly different lattice parameters. Indeed, Ga atoms trapped in the lattice induce an expanded unit cell volume which increases with the Ga content. This δ to α′ phase transformation shows unusual double-C curve kinetics in a time–temperature–transformation diagram (TTT). The occurrence of the double-C was attributed by Orme et al. [2] to a difference in isothermal mechanism: a massive transformation for the upper C and a martensitic transformation for the lower. Deloffre et al. [3,4] also investigated the nature of this isothermal martensitic transformation by X-ray diffraction (XRD), optical microscopy and dilatometry. For a gallium content lower than 1.5–1.6 at.%, the double-C behavior was attributed to the result of an indirect transformation, δ to α′ through a γ/γ′-phase (face-centered orthorhombic structure), for the upper C and a direct transformation for the lower C. For higher gallium concentrations, the transformation for the lower and upper C is a direct δ to α′ transformation. In parallel, density functional theory calculations performed by Sadigh and Wolfer [5] highlighted the lowest relaxed volume and energy site when the Ga atom occupied the site eight (using Zachariasen and Ellinger's nomenclature [6]) of the monoclinic α′ structure. The position of Ga atoms in this specific site would explain the upper C. According to this assumption, the lower C would be the result of a random Ga distribution due to the limitation of the diffusion process. However, this assumption has not yet been experimentally verified. More recently, in order to characterize the orientation relationship, parent–product interface at the atomic level, habit plane, twin relationship and plastic deformation of δ to α′ martensitic transformation, analyses were performed using transmission electron microscopy by Moore et al. [7]. The results showed the coexistence in the δ-phase of two habit planes (1 1 1) and (1 2 3), previously determined by Zocco et al. [8]. Thus, these habit planes might also correspond to both noses observed in the TTT diagram of PuGa alloys.

The thermodynamic δ to α′-phase transformation, and its reversion, were studied by Blobaum et al. [9] and by Oudot et al. [10] using a differential scanning calorimeter. On the one hand, the results obtained suggested that the embryos of the martensitic

* Corresponding author. Tel.: +33 3 80 23 46 39; fax: +33 3 80 23 52 17.
E-mail address: brice.ravat@cea.fr (B. Ravat).

0022-3115/$ - see front matter © 2009 Elsevier B.V. All rights reserved.
doi:10.1016/j.jnucmat.2009.06.028

transformation could be the result of the δ-phase eutectoid decomposition. On the other hand, in addition to the double-C behavior, a third distinct thermal process was observed that could be the result of a number of possibilities such as microstructure, composition, crystalline phase, intermediate products, etc. To summarize, over the last forty years, different theories or hypotheses have been suggested to explain the martensitic transformation as well as the double-C behavior but their fundamental origin still remains poorly understood.

Experimental data, resulting from direct martensitic transformation investigations at low temperature, remain uncommon. Indeed, only the neutron diffraction experiment at low temperature carried out by Lawson et al. on ^{242}PuGa alloys to characterize the lattice constants and anisotropic microstrain has been reported [11]. Until now, the main available structural data have been collected at room temperature or at higher temperature during the α'–δ reversion. Thus, in order to give rise to a better understanding of transformation mechanisms, a specific tool was developed at the CEA–Valduc to perform X-ray diffraction analyses at low temperature in a glove box.

The purpose of this work is to precisely study the martensitic transformation of a plutonium–gallium alloy including the nature and the amount of crystalline phases, as well as the microstructure, during a sub-ambient isothermal hold. Details on the experimental device and data collection are reported in Section 2, and the results are presented and discussed in detail in Section 3.

2. Experimental details

2.1. Samples description

This work was performed on a PuGa alloy with a gallium content of 2 at.% and 0.1 at.% of other so-called "δ-phase stabilizer" elements (Pu–2.1%$\Sigma\delta$-elets). This alloy was heated for 700 h at 460 °C under high vacuum condition (2×10^{-7} mbar) to fully homogenize the gallium distribution. Samples with dimensions of 10 mm diameter and 0.3 mm height were obtained by microcutting. Annealing at 360 °C for 6 h was used to restore the crystalline structure. Finally, to remove surface oxides, samples were electropolished at a voltage of 40 V in a cooled bath (90% ethylene glycol and 10% nitric acid) at a temperature of −10 °C.

2.2. Experimental device

In order to perform XRD experiments at different temperature, a temperature chamber (TTK 450 Anton Paar) was mounted on a θ/θ goniometer (Fig. 1). The temperature ranges from −193 to 450 °C using a heating/cooling block located inside the chamber. The heating/cooling block was cooled down with a circulating liquid nitrogen supply and heated with a resistive heater. The sample holder, which has positioned on the heating/cooling block is made of copper and is chromium-plated that provides outstanding heat conductivity and high corrosion resistance. The heat transmission was ensured by applying a heat conducting paste onto the sample holder. The temperature was regulated by a thermocouple which was inserted on the front surface of the sample holder for a high-precision measurement and control of the working temperature.

The diffractometer used was a classical θ/θ diffractometer (BRUKER AXS D8 Advance) with Cu Kα tube which was set to 40 kV and 40 mA with an X-ray beam energy of 8.048 keV. Analyses are performed in Bragg–Brentano geometry. To improve the counting time, the detector used was a high speed positive sensitive detector (BRUKER AXS VANTEC), integrating over an angular range of 6°, with a 12 μm thick nickel foil used to remove the K_β radiation. In order to have the best compromise between the counting time and the angular resolution, a slit with a width of 0.6 mm, which limits the beam divergence of the primary radiation beam, was used.

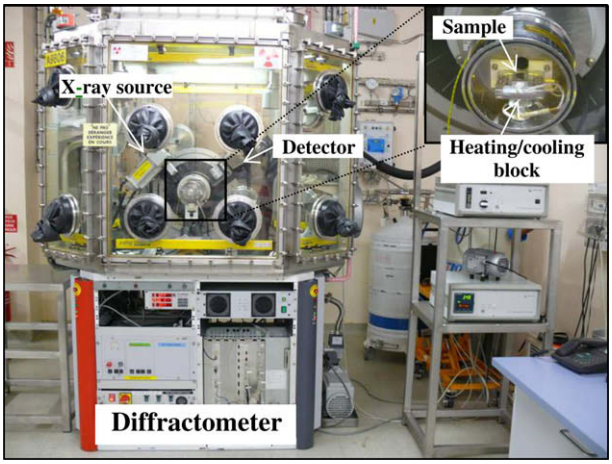

Fig. 1. Experimental device developed at the CEA–Valduc, which is dedicated to XRD experiments on plutonium alloys at different temperatures.

The diffractometer coupled to the temperature chamber was modified to be placed in a glove box in order to account for all the safety elements required to analyze plutonium alloys at temperature using X-rays.

2.3. Experimental details and data collection and analysis

The sample was cooled down from room temperature to −130 °C, with an average cooling rate of about 30 K min^{-1}, and held for 48 h in order to characterize the δ–α' phase transformation in the upper C. The choice of the temperature of −130 °C was motivated by the fact that this temperature corresponds to the nose of the upper C and, consequently, to a maximum of δ–α' transformation for an homogenized PuGa alloy with a gallium content of 1.9 at.% according to the TTT diagram published by Orme et al. [2], as shown in Fig. 2. Before cooling down the sample, a conditioning time at room temperature greater than 6 h was respected. Indeed, regarding Blobaum et al. work, this conditioning time is necessary to ensure a maximum of transformation [9]. The diffraction patterns were recorded with a step time of 0.1 s and a step size of 0.015° from 27° up to 122° in 2θ angle. Before and after the

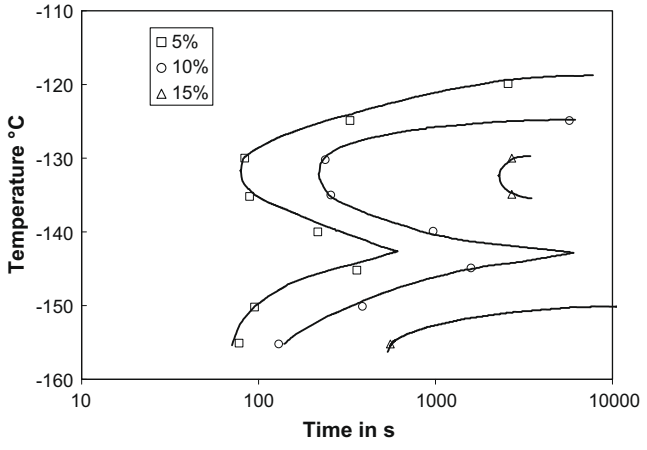

Fig. 2. Time–temperature–transformation δ to α'-phase diagram for a Pu–1.9 at.% Ga alloy (data published by Orme et al. [2]).

experiments series, the calibration of the experimental device was verified using a NIST Silicon standard (Si 640c) and the instrumental resolution function was determined using a LaB_6 powder standard (NIST SRM 660a). The LaB_6 powder pattern, which is a supposed perfect polycrystalline powder (no size and strain broadening compared to instrumental broadening), was refined using the Thompson–Cox–Hastings (TCH) pseudo-Voigt profile function [12]. The fitted values of the TCH function for LaB_6 giving the instrumental broadening are $U = 0$, $V = 6.36 \times 10^{-4}$, $W = 3.51 \times 10^{-4}$, $X = 5.22 \times 10^{-3}$, $Y = 4.28 \times 10^{-2}$.

In order to analyze the recorded diffraction patterns via full-pattern Rietveld refinement, the Fullprof program [13] was used. During all the Rietveld refinements, atoms positions were fixed for the δ and α' phases according to Zachariasen and Ellinger [6] and the refined parameters included the diffuse background, the sample displacement, the scale factor, the Debye–Waller factor and the lattice parameters. For the peak profile refinement, two different strategies were used. A pseudo-Voigt function was chosen to evaluate the α'-phase amount, whereas the anisotropic peak shape function, which is described with more details in Section 3.1, was used for the anisotropic microstrain and the crystallite size analysis.

3. Results and discussion

3.1. Observed diffraction patterns

Typical X-ray diffraction patterns of the sample at room temperature and after an isothermal hold at −130 °C for 48 h are gathered in Fig. 3. The diffraction patterns highlight that the martensitic transformation is the result of a direct $\delta \rightarrow \alpha' + \delta$ phase transformation which is in good agreement with Deloffre's work on PuGa alloys with a gallium content higher than 1.6 at.% [3–4]. Indeed, no diffraction peaks corresponding to γ/γ'-phase were observed. The α'-phase amount was calculated from the fitted diffraction patterns using Rietveld method. The total amount of the α'-phase precipitated after the isothermal exposure at −130 °C was determined at about 27%. Moreover, a significant peak broadening of the δ phase was observed at low temperature for all Bragg's peaks. This can be induced by the development of strong microstructural modifications of the δ phase induced by the 19% volume difference between the δ and α' phases. The α'-phase growth mechanism as well as the microstrain induced on the host δ phase are analyzed in detail in the next parts.

3.2. Microstructural analysis

3.2.1. Analysis method

The broadening of the Bragg's peaks profile depends on the microstructure of the analyzed material and, more particularly, on the finite crystallite size and cell strain [14]. To characterize these features, Rietveld refinement of the diffraction patterns can use isotropic or anisotropic models. Then, it can distinguish the size and strain effects through their different dependence on the d_{hkl} lattice spacing. The broadening models used, adapted to the cell symmetry, which are included in the Fullprof program, are based on the formalism developed by Stephens [15] for the anisotropic microstrain analysis and based on a spherical harmonics development for the crystallite size analysis as suggested in the Popa's model [16].

Peak broadening due to the finite crystallite size is evaluated by a very general phenomenological model, using the Scherrer formula, which considers that the size broadening can be written as a linear combination of spherical harmonics, as shown in the Eq. (1). In the used refinement process, the size effects were supposed to affect only the Lorentzian component of the peak:

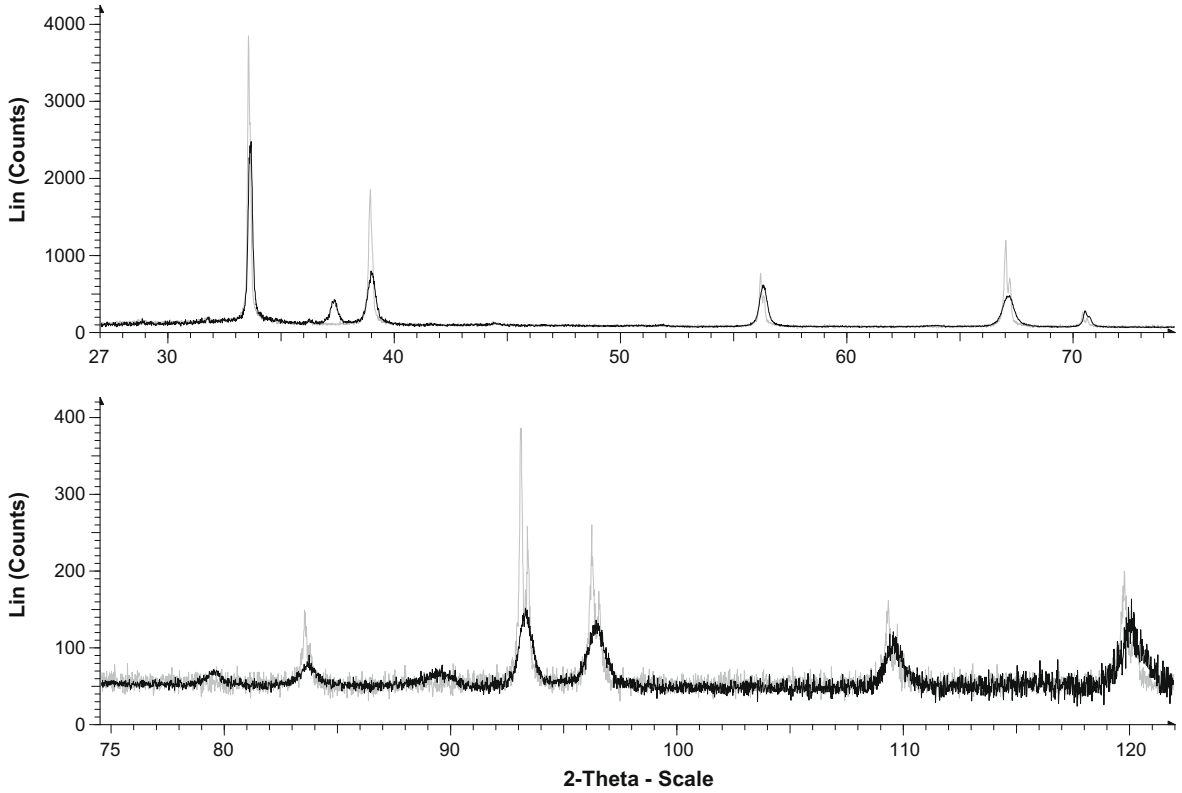

Fig. 3. X-ray diffraction patterns recorded for Pu−2.1%Σδ-elets at room temperature (in grey) and at −130 °C after an isothermal hold for 48 h (in black) showing the occurrence of the α'-phase and the broadening of the Bragg's peaks of the host δ-phase.

$$\beta_{hkl} = \frac{\lambda}{D_{hkl}\cos\theta} = \frac{\lambda}{\cos\theta}\sum_{l,m} C_{l,m} Y_{l,m}\left(\theta_{h,k,l}, \varphi_{h,k,l}\right), \quad (1)$$

D_{hkl} corresponds to the apparent size in the [hkl] direction, β is the peaks integral breadth, $C_{l,m}$ are the spherical harmonics coefficients, $Y_{l,m}$ are the spherical harmonics functions [17] and θ and ϕ give the direction in reciprocal space.

Otherwise, the Stephens model was used to analyze the anisotropic microstrain. The contribution of the microstrain to peak broadening was selected as pure Gaussian (the Gaussian/Lorentzian ratio parameter was fixed to 0 to avoid calculation divergence). The microstrain is calculated using the following quadratic relationship:

$$\sigma^2\left(1\Big/d_{hkl}^2\right) = \sum_{HKL} S_{HKL} h^H k^K l^L \quad \text{with} \quad H+K+L=4, \quad (2)$$

σ^2 is the normalized variance, d_{hkl} the lattice plane spacing and the S_{HKL} coefficients depend on the crystal symmetry. As PuGa alloys crystallize in the cubic space group Fm3m, only two parameters, S_{400} and S_{220}, are necessary to refine the anisotropic strain broadening.

The determination of all these parameters allows the crystallite shape as well as the average cell microstrain versus orientation in the crystal space to be characterized.

3.2.2. Results and discussion

Rietveld refinements taking into account the microstructural models for the δ phase were performed on the diffraction patterns recorded at room temperature before cooling down and at the end of the isothermal hold at −130 °C in order to investigate the stress induced by the production of α' phase on the microstructure of the δ matrix. After several refinement attempts, the size was eventually supposed to be anisotropic until the 4th order in the harmonic development. Indeed, on the one hand the refinement of K_{00} and K_{41} (coefficient of the spherical harmonic functions in the cubic symmetry) indicated a wide crystallite, meaning that it did not really contribute to the total broadening. On the other hand, the refinement of the 6th order anisotropic size parameters did not significantly improve the Rietveld refinement (the weighted profile factor R_{wp} before and after transformation was respectively 0.1% and 0.5%) and furthermore did not lead to a physical representation of apparent size. This result on the crystallite size did not allow a quantitative analysis of the calculated size values. We can only highlight that the crystallite size is about equal before and at the end of the transformation. Even if the R_{wp} factor seems to be important (cf. Table 1), it is mainly induced by the weak counting statistic. This does not influence the quality of the refinement since the refined pattern fit well the peaks shape of the δ-phase. Typical refined diffraction patterns are presented in Fig. 4. The results of the Rietveld refinement as well as the deduced values of anisotropic size and microstrain are summarized in Table 1. Thanks to the determination of anisotropic microstrain coefficients (S_{400} and S_{220}), δ-phase microstrain 3D representations of analyses performed at room temperature (i) and at the end of the isothermal hold at −130 °C (ii) (with the presence of α'-phase) could be calculated and are shown in Fig. 5. The results show that after the phase transformation the average strain is clearly higher at low temperature and multiplied by a factor of about 8. Indeed, the microstrain in the alloy stabilized in the mono δ-phase is weak (from 3.14×10^{-4} to 3.90×10^{-4}), but the appearance of the α' phase induced a large amount of microstrain in the δ matrix (from 13.27×10^{-4} to 42.34×10^{-4}). Moreover, a microstrain maximum occurred in the [1 0 0] direction whereas the minimum was observed in the [1 1 1] direction (i.e. in the direction with high atom density). The anisotropic elastic response of each crystallite is the result of the surrounding stress and the elastic single crystal constants, which are for the Pu δ-phase the most anisotropic of all the fcc metals. Thus, this microstrain can be related to the stiffness of the crystallographic direction. The results are also in good agreement with the microstrain determined by Lawson et al. [11] on ^{242}PuGa alloys using neutron diffraction at low temperature. Indeed, the same microstrain anisotropy was found. However, the microstrain values determined in this work are about twice those calculated by Lawson. This increase in stress applied to the δ matrix can be explained by the difference of the observed amount of α'-phase present in these samples. Indeed, whereas the anisotropic microstrain was calculated in this work for an amount of α'-phase of about 27%, no α'-phase transformation was detected at low temperature by Lawson. Thus, the occurrence of microstrain was explained by the development of α' nuclei which created a spatially inhomogeneous stress distribution in the δ matrix.

Furthermore, the difference in the microstrain observed versus the crystallographic orientation direction may be also related to δ to α'-phase transformation. Indeed, according to the Hecker et al. review [18], the orientation relationships of the α' and δ-phases, in the martensitic transformation process, are close to the following:

$$(1\,1\,1)_\delta \,||\, (0\,2\,0)_\alpha \quad \text{and} \quad [\bar{1}\,1\,0]_\delta \,||\, [1\,0\,0]_\alpha.$$

The $(1\,1\,1)_\delta$ plane can be considered as the invariant plane and the $[1\,1\,1]_\delta$ direction is the directional growth of the α'-phase. The α' plate contained in the δ matrix is composed of two alternative twin variants that share a common $[0\,2\,0]_\alpha$ direction but differ by a 60° rotation. The $(2\,0\,5)_\alpha$ twinning is the lattice invariant deformation mode, as revealed by transmission electron microscopy [7]. Thus, as the martensitic transformation process does not directly distort

Table 1
Results of the Rietveld refinement of the diffraction patterns of the Pu−2.1%Σδ-elements recorded at room temperature before cooling down and after an isothermal hold at −130 °C of 48 h, as well as the deduced values of size and microstrain.

	Room temperature	After hold at −130 °C (48 h)
Phases in sample	δ	δ(73%) and α(27%)
R_{wp} (in%)	29.7	41.3
R_{Bragg} (δ-phase)	7.9	7.1
a (in Å)	4.62605 ± 0.00004	4.62264 ± 0.00019
K_{00} (in Å^{-1})	$0.94\ (\pm0.03)\times10^{-3}$	$0.91\ (\pm0.12)\times10^{-3}$
K_{41} (in Å^{-1})	$0.34\ (\pm0.05)\times10^{-3}$	$0.42\ (\pm0.16)\times10^{-3}$
Average apparent size	1067 ± 34 Å	1096 ± 138 Å
S_{400} (in Å^{-4})	$3.32\ (\pm1.52)\times10^{-10}$	$3.93\ (\pm0.28)\times10^{-8}$
S_{220} (in Å^{-4})	$3.15\ (\pm3.56)\times10^{-10}$	$-2.77\ (\pm0.39)\times10^{-8}$
Average maximum strain	3.46×10^{-4}	26.94×10^{-4}
Maximum strain value	$3.90\ (\pm0.90)\times10^{-4}$ in [2 0 0]	$42.34\ (\pm1.49)\times10^{-4}$ in [2 0 0]
Minimum strain value	$3.14\ (\pm1.24)\times10^{-4}$ in [1 1 1]	$13.27\ (\pm3.81)\times10^{-4}$ in [1 1 1]

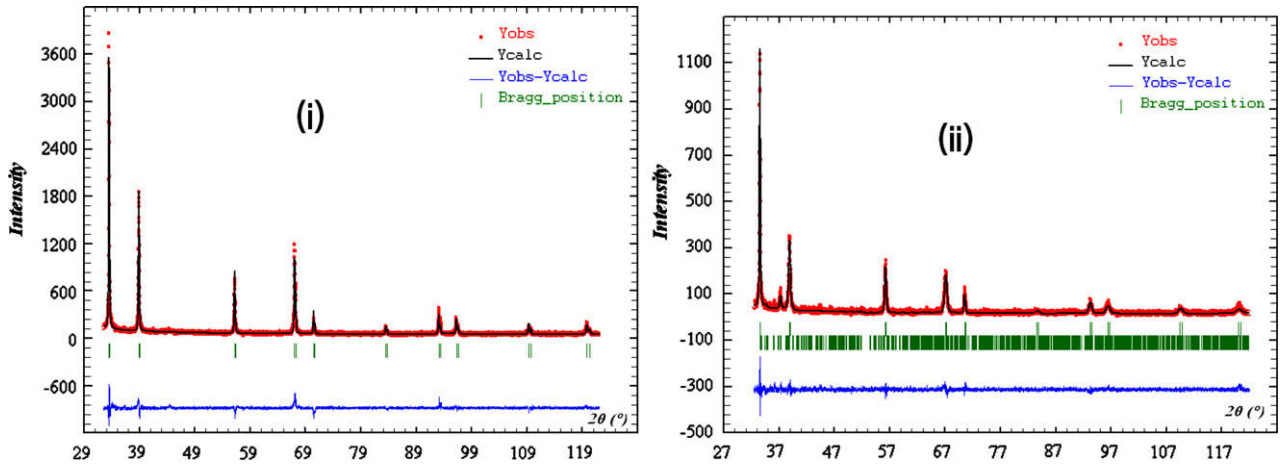

Fig. 4. Rietveld refined diffraction patterns of the Pu–2.1%Σδ-elets recorded at room temperature before (i) cooling down and (ii) after an isothermal hold at −130 °C of 48 h.

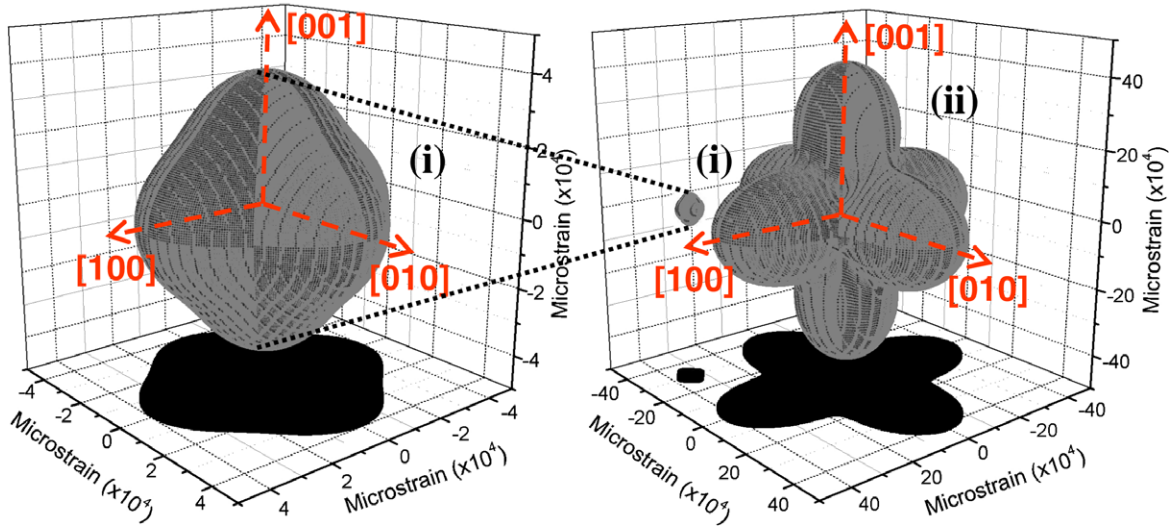

Fig. 5. Anisotropic microstrain 3D representations of the δ-phase calculated for the Pu–2.1%Σδ-elets: (i) at room temperature and (ii) at the end of the isothermal hold at −130 °C (with the presence of the α′-phase).

the $(1\,1\,1)_\delta$ plane, this may also explain why the microstrain amount is the lowest in the $[1\,1\,1]_\delta$ direction. Nevertheless, an increase in microstrain after the martensitic transformation in this $[1\,1\,1]_\delta$ direction is observed all the same. As discussed before, it should result from the microstress development induced by the 19% volume difference between the δ and α′-phases.

3.3. Kinetic study of the $\delta \rightarrow \alpha' + \delta$ phase transformation

3.3.1. Analysis method

In order to characterize the nucleation process during the $\delta \rightarrow \alpha'$ transformation, the precipitation kinetics was analyzed in situ during the isothermal hold at −130 °C by X-ray diffraction. Then, Rietveld refinements were performed on the recorded diffraction patterns to determine the α′-phase amount as a function of time. Analysis of the amount of the α′-phase evolved was made within the framework of the Avrami theory by means of the Johnson–Mehl–Avrami–Kolmogorov (JMAK) equation [19–23]. Eq. (3) describes the kinetics of the transformation giving a relation between the fraction of transformed material and time. For isothermal transformations, this equation has the following form:

$$f = 1 - e^{-k \cdot t^n}, \tag{3}$$

where f is the product volume fraction which varies versus time (t) in seconds, k the reaction rate constant and n the Avrami index that describes the nucleation and growth mechanisms. In this work, the classic JMAK theory was adapted to model the kinetics of the $\delta \rightarrow \alpha' + \delta$-phase transformation in PuGa alloys. Thus, Eq. (3) can be written in the form:

$$f_{\alpha'}(t)/f_{\alpha'}^{\max} = x(t) = 1 - e^{-k \cdot t^n}, \tag{4}$$

where $f_{\alpha'}(t)$ is the amount of α′-phase after a time t, $f_{\alpha'}^{\max}$ is the maximum (equilibrium) volume fraction of the α′-phase at the temperature of the transformation and $x(t)$ is the degree of the transformation.

It must be pointed out that the JMAK equation describes only the transformation from its start and does not consider the preprocessing stages corresponding to the embryos formation and the incubation time.

3.3.2. Results and discussion

The amount of α′-phase evolved, as deduced from Rietveld refinement versus time, is shown in Fig. 6. Eq. (4) was used to analyze the experimental data by means of logarithmic plots as shown in Fig. 7, where $\ln(-\ln(1-x(t)))$ is plotted versus $\ln(t)$ allowing the

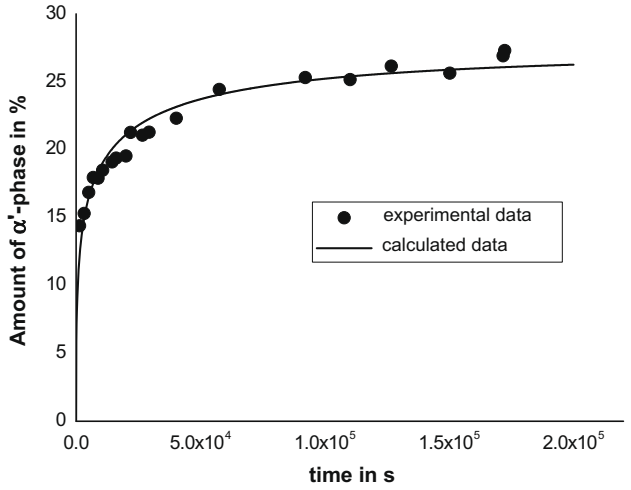

Fig. 6. Experimental and calculated amount of the α'-phase describing the kinetics of the $\delta \rightarrow \alpha'$ transformation at −130 °C.

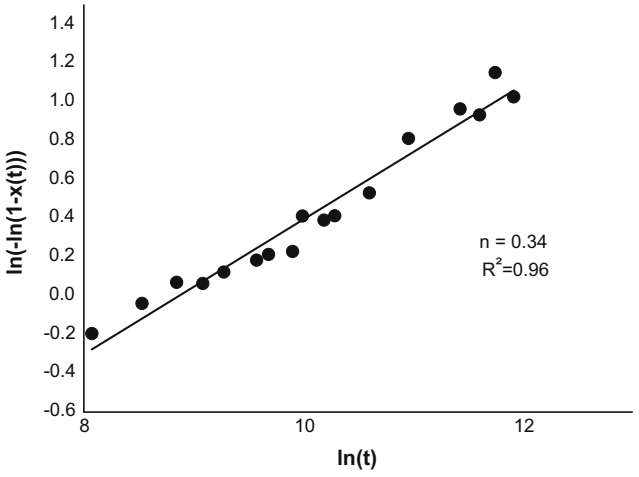

Fig. 7. Plots of $\ln(-\ln(1-x(t)))$ versus $\ln(t)$ to allow the determination of the JMAK parameters at −130 °C.

Avrami exponent n (slope of the resulting linear fit) to be determined, as well as the reaction rate constant k (y axis-intercept). The results show that the experimental measurements are well described by a linear fit ($R^2 = 0.96$). This means that the JMAK theory can be applied to describe the kinetics of the $\delta \rightarrow \alpha' + \delta$-phase transformation in Pu−2.1%$\Sigma\delta$-elets alloy under isothermal conditions. Moreover, the transformation mechanism did not seem to change during the transformation.

The Avrami coefficient, n, depends on both nucleation and growth mechanisms. Therefore, knowledge of n is helpful in order to understand the phase transformation process at a given temperature. The n exponent value, obtained for the isothermal hold at −130 °C is 0.34. This value corresponds to a general mechanism where δ-grain edges are the nucleation sites and the α'-phase has a plate-like morphology [24].

Similar observations were reported for stainless steels (316SS) [25] or for β titanium alloys (Ti 10–2–3 and β-CEZ) [26] corresponding to the later transformation regimen and occurring after a rapid precipitation regimen. Through analogy with these alloys, we suggest for δ-Pu alloy at low temperature, that the $\delta \rightarrow \alpha' + \delta$ transformation may consist of a quick nucleation at grain boundaries [27] in the first regimen and this is followed by a slow interface growth mechanism which controls the thickness of large α' plates.

The derived JMAK parameters allow the transformation kinetics to be calculated at −130 °C. In Fig. 6, the calculated (using JMAK theory) and the experimental kinetics were compared. Calculated fractions were based on Eq. (2) using n and k obtained values. Very good agreement between the calculated and the experimental curves was found indicating the accuracy of the JMAK kinetic parameters obtained.

4. Conclusion

The modifications of the microstructure were characterized using X-ray diffraction at low temperature. Thus, in order to investigate the martensitic transformation, an isothermal hold at −130 °C for 48 h was performed on a highly homogenized PuGa alloy. The analysis of the recorded diffraction patterns highlighted a direct and incomplete $\delta \rightarrow \alpha' + \delta$-phase transformation. The appearance of the α'-phase induced important microstructural modifications, in the δ matrix, resulting from the stress induced by a cell volume difference of 19% between the δ and α'-phases. Indeed, anisotropic microstrain in the δ-phase was determined and showed a microstrain maximum in the [1 0 0] direction and a minimum in [1 1 1] during the $\delta \rightarrow \alpha'$-phase transformation.

The amount of α'-phase evolved was analyzed within the framework of the Avrami theory in order to characterize the nucleation process. The results suggested that the growth mechanism corresponded to a general mechanism where δ-grain edges were the nucleation sites and the α'-phase had a plate-like morphology.

To conclude, these promising results have highlighted the potential of the new experimental device, developed at the CEA–Valduc, to analyze the crystalline structure of plutonium alloys as a function of temperature.

Acknowledgements

We wish to thank P. De Boissieu and M. Nadisic for their precious contribution to the development of the experimental device as well as for their participation in sample preparation and experimental achievements.

References

[1] N.T. Chebotarev, E.S. Smotriskaya, M.A. Andrianov, O.E. Kostyuk, Plutonium and Other Actinides, vol. 37, North-Holland Publishing Company, 1976.
[2] J.T. Orme, M.E. Faiers, B.J. Ward, Plutonium and Other Actinides, vol. 761, North-Holland Publishing Company, 1976.
[3] P. Deloffre, J.L. Truffier, A. Falanga, J. Alloy Compd. 271–273 (1998) 370.
[4] P. Deloffre, Ph.D. Thesis, University of Paris, France, 1997.
[5] B. Sadigh, W.G. Wolfer, Phys. Rev. B72 (2005) 205122.
[6] W.H. Zachariasen, F.H. Ellinger, Acta Crystallogr. 16 (1963) 777.
[7] K.T. Moore, C.R. Krenn, M.A. Wall, A.J. Schwartz, Metall. Mater. Trans. A 38 (2007) 212.
[8] T.G. Zocco, M.F. Stevens, P.H. Adler, R.I. Sheldon, G.B. Olson, Acta Metall. Mater. 38 (11) (1990) 2275.
[9] K.J.M. Blobaum, C.R. Krenn, M.A. Wall, T.B. Massalski, A.J. Schwartz, Acta Mater. 54 (2006) 4001.
[10] B. Oudot, K.J.M. Blobaum, M.A. Wall, A.J. Schwartz, J. Alloy Compd. 444–445 (2007) 230.
[11] A.C. Lawson, J.A. Roberts, B. Martinez, R.B. Von Dreele, B. Storey, H.T. Hawkins, M. Ramos, F.G. Hampel, C.C. Davis, R.A. Pereyra, J.N. Mitchell, F. Freibert, S.M. Valone, T.N. Claytor, D.A. Viskoe, F.W. Shonfeld, Philos. Mag. 85 (18) (2005) 2007.
[12] P. Thompson, D.E. Cox, J.B. Hastings, J. Appl. Crystallogr. 20 (1987) 79.
[13] J. Rodriguez-Carvajal, M.T. Fernandez-Diaz, J.L. Martinez, J. Phys.: Condens Matter 3 (19) (1991) 3215.
[14] E.F. Bertaut, C.R. Acad. Sci. Paris 228 (1949). 187 and 492.
[15] P.W. Stephens, J. Appl. Crystallogr. 32 (1999) 281.
[16] N.C. Popa, J. Appl. Crystallogr. 31 (1998) 176.
[17] M. Jarvinen, J. Appl. Crystallogr. 26 (1993) 527.
[18] S.S. Hecker, D.R. Harbur, T.G. Zocco, Prog. Mater. Sci. 49 (2004) 429.

[19] A.N. Kolmogorov, Izv. Akad. Nauk. SSR 3 (1937) 355.
[20] M. Avrami, J. Chem. Phys. 7 (1939) 1103.
[21] M. Avrami, J. Chem. Phys. 8 (1940) 212.
[22] M. Avrami, J. Chem. Phys. 9 (1941) 177.
[23] W.A. Johnson, R.F. Mehl, Trans. Am. Inst. Min. Metall. Eng. 135 (1939) 416.
[24] J.W. Christian, The Theory of Transformations in Metals and Alloys, Part 1, second ed., Pergamon Press, Oxford, 1975.
[25] G. Sasikala, S.K. Ray, S.L. Mannan, Mater. Sci. Eng. A359 (2003) 86.
[26] S. Bein, J. Bechet, J. Phys. IV 6 (1996) C1.
[27] S. Hecker, JOM 55 (9) (2003) 13.